

# Tension–tension fatigue failure behaviour of poly(phenylene ether ketone) (PEK-C)

Jiang Zhou\*†, Alberto D'Amore‡, Guoqing Zhuang†, Tianbai He†, Binyao Li† and Luigi Nicolais‡

†Polymer Physics Laboratory, Changchun Institute of Applied Chemistry, Chinese Academy of Sciences, Changchun 130022, P. R. China and ‡Department of Materials and Production Engineering, University of Naples, Piazzale Tecchio 80, 80125 Napoli, Italy  
(Received 15 March 1995; revised 22 August 1995)

Tension–tension fatigue tests were conducted on unnotched injection moulded poly(phenylene ether ketone) (PEK-C) specimens with two stress ratios,  $R$ . The fatigue behaviour of this material is described. The  $S$ – $N$  curves ( $S$  = alternating stress,  $N$  = number of cycles to failure) for different  $R$  values have the same general shape, but the curve for bigger  $R$  is shifted to long cycles. A fatigue lifetime inversion is observed from constructed  $S$ – $N$  curves. Examinations of failure surfaces and analyses of the fatigue data reveal that the fatigue failure mechanism of the material studied is crack growth dominated. But the manner of the fatigue crack initiation and propagation depends on the maximum cyclic stress applied. At higher stresses, the fatigue crack originates at the corner of the specimen and propagates inward; at lower stresses, the fatigue crack nucleates at an internal flaw of the specimen and propagates outward. The fatigue lifetime inversion corresponds to the transition of crack initiation and propagation from one mode to the other.

Copyright © 1996 Elsevier Science Ltd.

(Keywords: tension–tension fatigue; injection moulded; poly(phenylene ether ketone))

## INTRODUCTION

High performance thermoplastics, as engineering plastics or as matrices for advanced composites, have been greatly developed in the past decades. This was in response to the demand for easily processed polymers which matched the strength and stiffness of thermosets and were able to provide improved temperature capability and chemical resistance compared with current thermoplastics. These high performance thermoplastics are being used more and more often for applications where considerable and repeated loading is involved. There is thus a need to acquire a better understanding of the fatigue performance and failure mechanisms of these materials under conditions of cyclic loading, and this is an essential prerequisite for these materials to be used reliably, safely and efficiently in service applications.

The traditional approach is investigating the fatigue behaviour to engineering plastics involves constructing an  $S$ – $N$  curve (the plot of the alternating stress  $S$  as a function of the number of cycles to failure  $N$ ) and determining the endurance limit (a stress threshold below which fatigue failure does not occur)<sup>1–3</sup>. However, the presence of inherent defects in materials is not taken into consideration in this approach. Inherent defects inevitably exist in materials and their geometry, size and orientation are random. Under fatigue loading, these defects undergo a complex process of growth and interaction and ultimately lead to the initiation of

macroscopic cracks. The propagation and coalescence of these cracks result in fatigue failure. This notion perhaps prompted another approach of researching the fatigue behaviour of engineering plastics, especially high performance thermoplastics, i.e. fatigue crack propagation analysis<sup>4–8</sup>. Through the application of fracture mechanics principles, this approach has become commonly used to estimate component lifetime in the situation where cracks or stress concentrations are known to be present. In spite of this, the  $S$ – $N$  approach is also a commonly accepted design criterion for fatigue resistance in engineering plastics. For example, ASTM method D671 for plastics specifies repeated flexural stress (fatigue) as a standard test.

Poly(phenylene ether ketone) (PEK-C) is an amorphous thermoplastic resin developed by Changchun Institute of Applied Chemistry, Chinese Academy of Science under Chinese Patent<sup>9</sup>. This high temperature resin possesses excellent physical and mechanical characteristics. In the past few years it has received extensive attention<sup>10–13</sup>. Although these studies provide a valuable insight into the behaviour of PEK-C, little is known, about its fatigue performance. Since PEK-C is a relatively new material, additional studies are needed in order to gain a deeper insight into its response to service conditions and to assess its potential applications. The primary purpose of this work is to extend the data available on PEK-C to include fatigue testing. Combining examination of failure surfaces, fatigue failure mechanisms under various loading conditions are also discussed.

\* To whom correspondence should be addressed

## EXPERIMENTAL

*Material and specimens*

The PEK-C resin used in this study was provided by Xuzhou Engineering Plastics Co. China. Its reduced viscosity in chloroform at 25°C is 0.5 dl g<sup>-1</sup>. Specimens were injection moulded using a JSW-17SA injection moulding machine with barrel temperature about 335°C. The specimen was a dumbbell-shaped ASTM D638 type I, end gated, with a gauge section 4.60 by 10.1 mm in cross-section. No attempt was made to smoothen the corners and surfaces of the specimens.

*Test method*

The tests were carried out under ambient conditions in a laboratory atmosphere. An Instron 8501 servohydraulic testing system was used to perform both static tensile and tension-tension fatigue tests. Specimen gripping was done with Instron wedge grips.

To establish fatigue cyclic stress levels, it is necessary to determine the ultimate tensile strength (UTS) of the material tested. Five specimens were tested to yield the average UTS. A cross-head speed of 100 mm min<sup>-1</sup> was used.

All fatigue tests were carried out under load control with a sinusoidal waveform. A range of frequencies

(0.98–2.00 Hz), which is low enough to avoid significant hysteresis heating, was used in generating *S-N* curves. The frequency was varied as a function of the maximum stress to maintain a constant load rate. Fatigue testing was done at several stress levels which were calculated on the basis of measured specimen dimensions relative to the UTS determined. These stress levels represented the proportion of UTS varying from 40 to 90%. The actual fatigue stress applied during a cycle may vary by a few per cent. Two minimum to maximum stress ratios, *R*, were used in the test, with values of 0.1 and 0.3. Tests were continued until the specimens broke.

The fracture surfaces after fatigue testing at different stress levels and stress ratios were inspected using a HITACHI S-570 scanning electron microscope to identify the failure mechanisms. All samples were sputter-coated with a thin layer of gold to improve sample conductivity.

## RESULTS AND DISCUSSION

*S-N data*

The tension-tension fatigue data for injection moulded PEK-C are listed in *Table 1*. Values are given for the maximum cyclic stress,  $S_{\max}$ , the ratio of  $S_{\max}$  to the measured UTS (for PEK-C UTS = 90.4 ± 3.78 MPa),

**Table 1** Tension-tension fatigue data for injection moulded PEK-C

$S_{\max}$ (MPa)	$S_{\max}/\text{UTS}$	$S_{\min}/S_{\max}$	Frequency (Hz)	Cycles to failure
81.36	0.9	0.1	0.89	661
81.36	0.9	0.1	0.89	3913
81.36	0.9	0.1	0.89	2147
72.32	0.8	0.1	1.00	7255
72.32	0.8	0.1	1.00	7850
72.32	0.8	0.1	1.00	4495
72.32	0.8	0.1	1.00	10 814
63.28	0.7	0.1	1.14	3608
63.28	0.7	0.1	1.14	5585
63.28	0.7	0.1	1.14	9248
54.24	0.6	0.1	1.33	6952
54.24	0.6	0.1	1.33	9080
45.20	0.5	0.1	1.60	32 872
45.20	0.5	0.1	1.60	16 888
36.16	0.4	0.1	2.00	25 019
36.16	0.4	0.1	2.00	55 519
81.36	0.9	0.3	0.89	6125
81.36	0.9	0.3	0.89	1369
81.36	0.9	0.3	0.89	3120
81.36	0.9	0.3	0.89	10 154
72.32	0.8	0.3	1.00	4024
72.32	0.8	0.3	1.00	15 493
72.32	0.8	0.3	1.00	10 158
63.28	0.7	0.3	1.14	9716
63.28	0.7	0.3	1.14	12 116
54.24	0.6	0.3	1.33	34 344
54.24	0.6	0.3	1.33	34 332
45.20	0.5	0.3	1.60	52 877
45.20	0.5	0.3	1.60	40 469
36.16	0.4	0.3	2.00	106 382
36.16	0.4	0.3	2.00	103 683

the minimum to maximum cyclic stress ratio,  $R$ , and the number of cycles at which the specimen failed. These data plotted into  $S-N$  curves in the form of maximum stress against the number of cycles to failure are shown in Figure 1. It can be seen from Figure 1 that each  $S-N$  curve has the same general shape, but the curve is shifted to long cycles with increasing stress ratio,  $R$ . At lower stresses (below 63.28 MPa), the data show typical fatigue lifetime behaviour with longer lifetimes at lower stresses,

and both curves are nearly linear and parallel to each other; the slopes of this portion of the curves appear to be independent of the  $R$  or insensitive to the change of  $R$ . At higher stresses (above 63.28 MPa maximum cyclic stress) an unusual inversion in fatigue lifetime can be observed, although it is not very obvious, where longer fatigue lifetime can be seen at higher stresses rather than at lower stresses. For example the lifetime at 72.32 MPa is longer than that at 63.28 MPa for  $R = 0.1$ . This lifetime inversion has been previously reported for BPA-polycarbonate<sup>14</sup> and polyestercarbonate<sup>15</sup> ASTM type tensile specimens with weld-line in the middle of the gauge length. This behaviour was explained by the presence of two separate fatigue lifetime branches, each branch corresponding to a distinct crack growth mode. A lifetime inversion was observed when a transition from one lifetime branch to the other occurred. For the material studied, the mechanisms dominating the fatigue lifetime inversion will be discussed later.

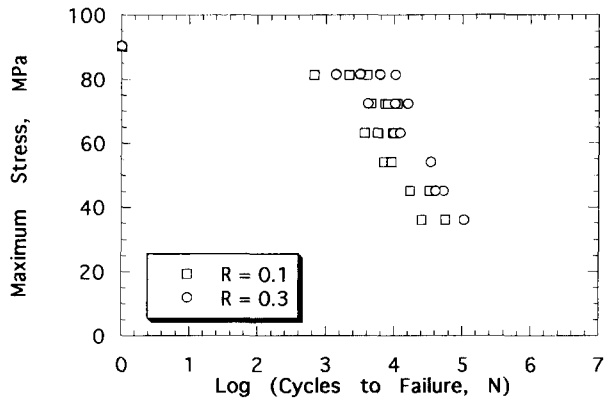


Figure 1 Tensile fatigue  $S-N$  curves for injection moulded PEK-C at different values of  $R$  (0.89–2.00 Hz)

### Fractography

In order to determine the similarity and differences of the failure mechanisms, it is necessary to inspect the fracture surfaces of the specimens tested at various stress levels. In all the tested specimens, two types of fracture surface features are observed. For the specimens tested under the conditions of maximum cyclic stress above 72.32 MPa when  $R = 0.1$  and at 81.36 MPa when

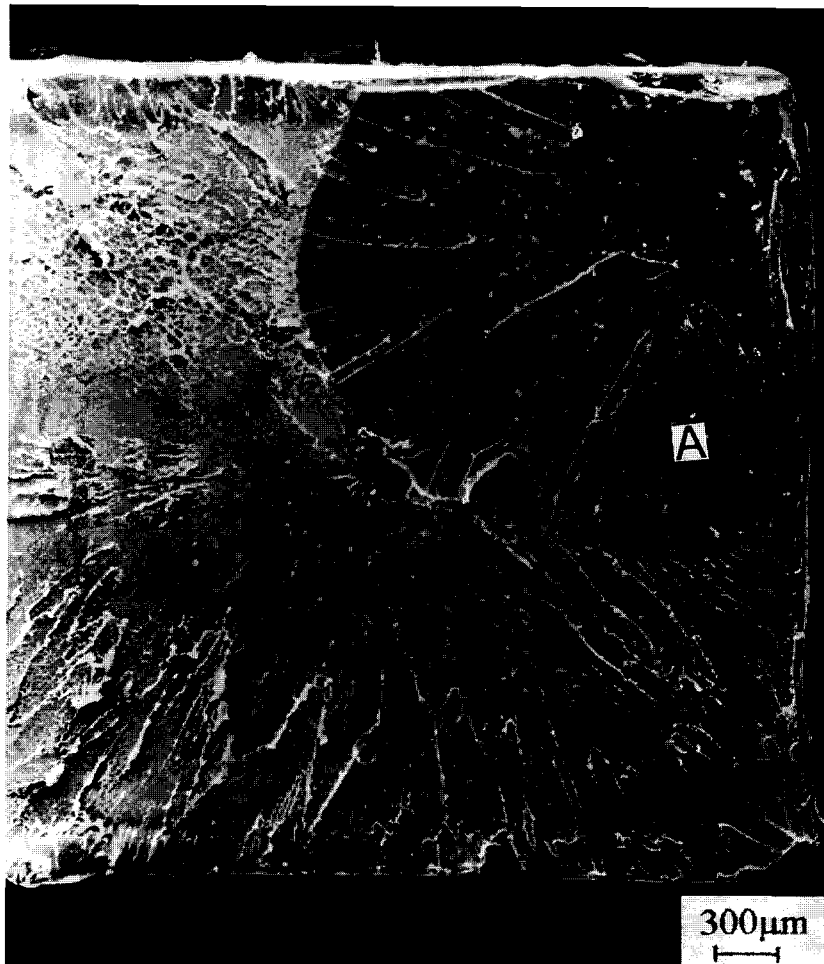


Figure 2 Fatigue fracture surface of injection moulded PEK-C,  $S_{max} = 0.8$  UTS,  $R = 0.1$



Figure 3 Higher magnification view of crack slow-growth region at point A of Figure 2

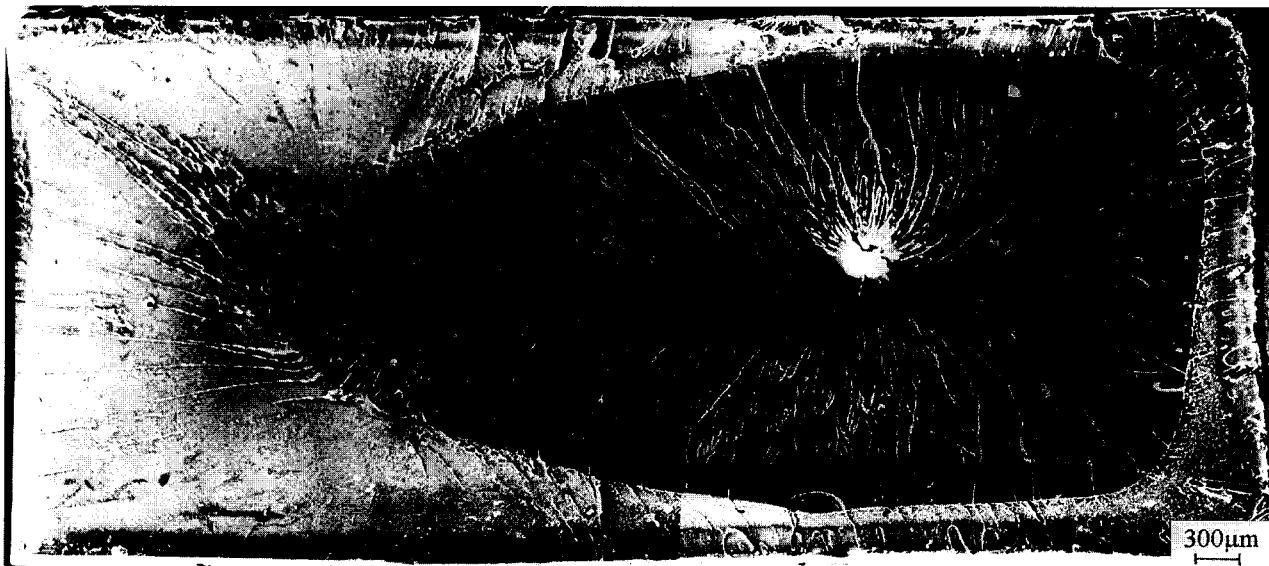


Figure 4 Fatigue fracture surface of injection moulded PEK-C,  $S_{max} = 0.5 UTS$ ,  $R = 0.3$

$R = 0.3$  (higher stress), the fracture surfaces have similar features, while for the specimens tested under the conditions of maximum cyclic stress below 63.28 MPa when  $R = 0.1$  and below 72.32 MPa when  $R = 0.3$ , the fracture surfaces have another alike morphology. The

micrography in Figure 2 shows part of a typical failure surface of a fatigue specimen tested at higher stresses. The entire fracture surface consists of two distinct zones, namely, a crack slow-growth region in one corner of the rectangular cross-section (the dark area at top right-hand

corner) and a rapid fracture region in the other area. In the crack slow-growth region, many concentric arched striations can be found. *Figure 3* is a micrograph at higher magnification taken from the area indicated by A in *Figure 2*. These striations represent a discontinuous propagation of the crack, and are marks of the position of the fatigue crack front. These observations indicate that at higher stresses, the fatigue crack nucleates at one corner of the rectangular cross-section, and propagates radially inward with the number of cycles, as is typical of fatigue crack growth, and eventually causes the fracture through unstable crack propagation. *Figure 4* is a typical micrograph of the fracture surface of a specimen tested at lower stresses. At first sight, it appears to be the failure surface of a fatigue specimen in which the fatigue crack originates at one of the shorter edges (right) of the rectangular cross-section, propagates with the number of cycles in a manner typical for fatigue crack growth, and finally results in fracture due to unstable crack propagation. However, careful examination shows that this is not true. In the fracture surface shown in *Figure 4*, there are small lips between the crack slow-growth region (dark area) and the edges of the rectangular cross-section of the specimen. Furthermore, the necked signs can also be found at the corresponding areas of these edges at the specimen surfaces. So, the fatigue crack seems to initiate in the specimen and grow outward. It is noted that there is a bright point at the central area of the slow-growth region. A higher magnification micrograph from this area (*Figure 5*) reveals that some circular striations surround this bright point which appears to be a flaw (inclusion). This examination shows that the flaw,

approximately 0.1 mm in size, is the origin of the fatigue crack. Similar initiation and growth of internal flaws in polymers were reported previously<sup>16,17</sup>. These inspections suggest that at low stresses, the fatigue crack originates at an internal defect of the specimen and propagates outward with the number of cycles until catastrophic failure results.

Summarizing the observations of fracture surface, it can be concluded that for the PEK-C, fatigue crack originates at the corner of the specimen and propagates inward at higher stresses, whereas at lower stresses, it nucleates at an internal flaw and grows outward. When the fatigue crack reaches a critical size at the corresponding stress level, it leads to rapid rupture. Similar results—fatigue cracks initiating at the corners at higher stresses and on internal flaws at low stresses—have been reported for as-moulded polysulfone<sup>18</sup>.

#### *Fatigue failure behaviour*

Although no damage monitoring techniques were employed during the fatigue tests, many microcracks oriented at 90° to the tensile direction could be observed by naked eye at the surfaces and corners of the specimens tested at high stresses. The higher the maximum cyclic stress applied, the greater in number and size are the microcracks. At lower stresses, no visible microcracks were found. These microcracks appeared to be crazes induced by higher stresses. *Figure 6* shows micrographs at higher magnification of the stable–unstable transition region at the fatigue fracture surfaces obtained under different loading conditions. Though the unstable growth region features with similar drawn honeycomb

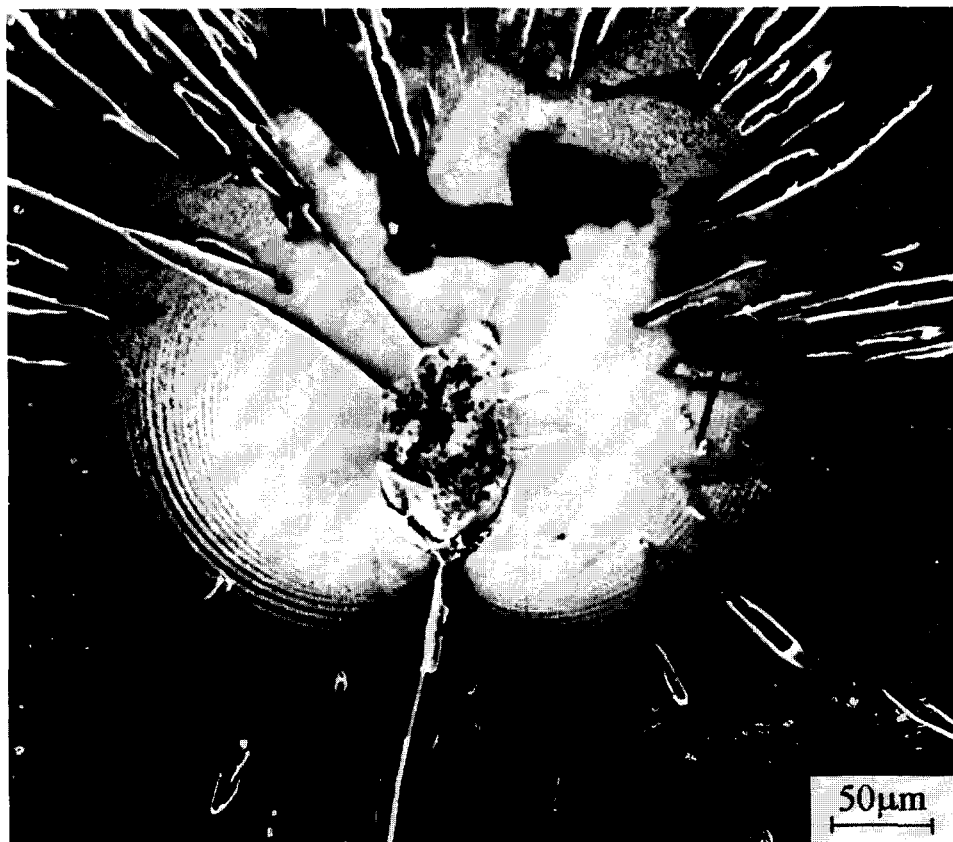


**Figure 5** Interior fatigue crack initiation at defect in injection moulded PEK-C,  $S_{max} = 0.5$  UTS,  $R = 0.1$



**Figure 6** Higher magnification view of the stable-unstable transition on the fatigue fracture surface. (a)  $S_{\max} = 0.9$  UTS,  $R = 0.1$ ; (b)  $S_{\max} = 0.4$  UTS,  $R = 0.1$ ; (c)  $S_{\max} = 0.5$  UTS,  $R = 0.3$

texture, it is clearly seen from low magnification view (Figures 2 and 4) that the amounts of surface roughness of the unstable crack growth region are different in these two cases. For the specimens in which the fatigue crack propagates inward (Figure 2), the fracture surface, especially near the edge of the specimen, shows more signs that the unstable crack growth region is not at the same plane. This suggests that the unstable crack growth may be the coalescence of isolated microcracks.

From the above observation and earlier discussion, one possible failure mechanism of PEK-C under tensile loading is proposed as follows. At high stress, microcracks formed at the surfaces and corners of specimens as a result of creep and yield, fatigue crack nucleated at one of these microcracks and propagated inward until unstable growth occurred. At low stress, the microcracks are too few to form a fatigue crack, therefore the fatigue crack is more likely to originate at internal defects of the specimen and grow outward until large enough to cause unstable fracture at the stress level used in the test.

As mentioned above, the failure mechanism of the material studied is dominated by fatigue crack growth, even if the manner of initiation and propagation of the fatigue crack is different. It is known that Paris's law gives a good description of fatigue crack growth behaviour not only in metals but also in polymers, described by the formula

$$da/dN = A(\Delta K)^m \quad (1)$$

where  $da/dN$  is the fatigue crack growth rate,  $\Delta K$  the stress intensity factor range from the minimum to maximum load, and  $A$  and  $m$  are constants dependent on the materials, environment, testing conditions, etc. If the lifetime of a specimen is dominated by fatigue crack growth, then it should be given approximately by the integration of equation (1) from the initial crack length to the length where the crack becomes unstable. However, this integration will be difficult because of the complex actual crack shapes and distributions in the specimen. But, based on equation (1), it may be assumed that

$$N \propto (\Delta S)^{-m} \quad (2)$$

where  $N$  is the specimen lifetime, and  $\Delta S$  is the stress range during each cycle. For the failure dominated by the fatigue crack growth, the bilogarithmic plot of  $\Delta S$  against  $N$  will give a linear curve with a slope  $1/m$ .

Figure 7 gives a representation of the data replotted in the form of stress range versus specimen lifetime for the two values of  $R$ . The data at shorter cycles (i.e. higher stresses) show larger scatter, but the data at longer cycles superimpose to form a single curve which is nearly linear. Linear regression analysis gives a gross exponent  $m = 4.5$  with a correlation coefficient of 0.8829 for all the data,

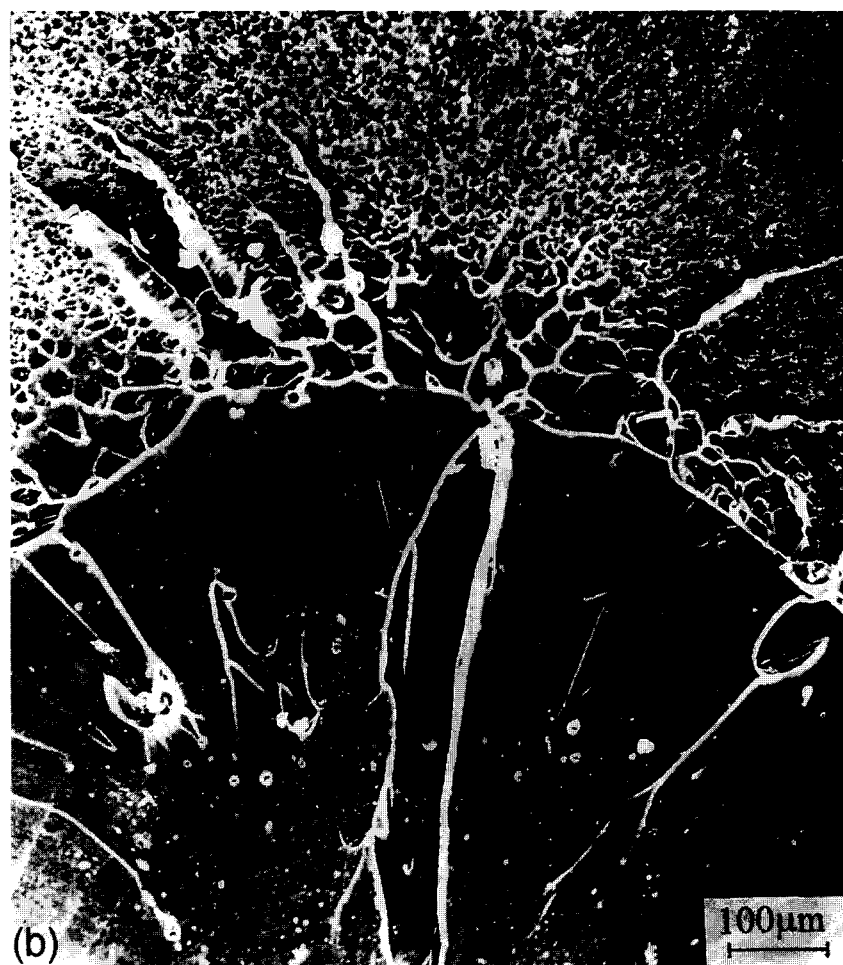


Figure 6 (Continued)

while the data at longer cycles yield a straight line having  $m = 4.2$  and correlation coefficient of 0.9310, as shown in Figure 7. This result is consistent with those reported for many polymers which have a value of  $m$  of approximately 4 (refs 1, 18, 19). The difference of scatter extent for the data at various stress levels in Figure 7 may reflect the difference of the failure mechanisms. It is known that the failure of the studied material is dominated by fatigue crack growth, but, many microcracks are formed in the specimen at higher stresses, the poor description given by equation (2) of fatigue behaviour is due to the complex shapes and distributions of these microcracks. On the other hand, there is only one main fatigue crack in each of the specimens tested at lower stresses, therefore equation (2) can describe fatigue behaviour better than it does at higher stresses.

It should be recognized that when equation (2) is used to predict the specimen lifetime, the process of the fatigue crack nucleation is not considered. The agreement of the data in Figure 7 with the expected relationship of equation (2), which is based on the fatigue crack propagation, suggests that the crack initiation stage is insignificant for the whole fatigue failure process, at least at lower stresses. However, the observations of crack initiation and propagation during tests and on fracture surfaces for polysulfone<sup>18</sup> do not support this conclusion. For the studied material, determination of the cycles required to initiate the fatigue crack is very difficult, and is not attempted in the work reported here.

In Figure 7, the fatigue lifetime inversion is still present, even if the inversion in number of cycles is not large and the transition spans a narrow range of stresses. It is notable that the stress range in which the fatigue lifetime inversion occurs is exactly the range at which the fatigue crack changes its initiation location from the corner to the interior of the specimen. As has been shown, there are two different crack initiation and growth modes for the studied material. The crack nucleated at the corner propagates radially inward in a range with  $\pi/4$  arc, while the crack nucleated in the interior propagates radially outward in any direction (in a range with  $2\pi$  arc). The initial size of the crack which will grow as the fatigue crack should be larger at lower stresses than at higher stresses, and the perimeter of the internal crack should be longer than the length of the crack front of the corner crack. Under the condition that the range of the stress intensity factor,  $\Delta K$ , is approximately the same, the fatigue crack growth rate is equal according to equation (1), but the fracture area created by internal fatigue crack propagation will be larger than that by corner fatigue crack propagation. This can make the lifetime of a specimen with an internal crack shorter than that of a specimen with a corner crack at the transition range of the two types of crack growth. Of course, the problem may not be so simple. The critical size of the fracture area in the specimen to cause catastrophic failure should be larger at low cyclic stress level compared with that at high cyclic stress level;



Figure 6 (Continued)

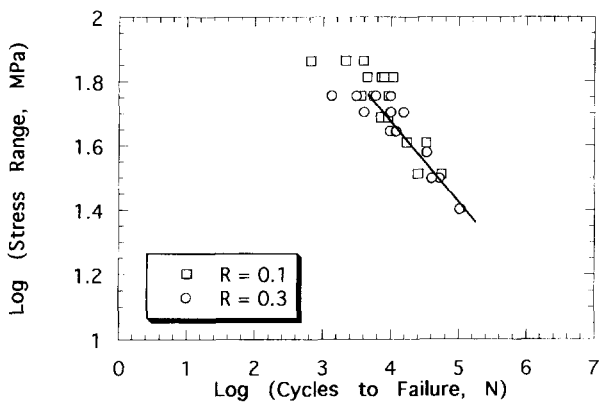


Figure 7 Fatigue data plotted as the stress range against lifetime

moreover, the crack initiation and fatigue crack growth may show different stress and time sensitivity for the two types. It is these factors that determine the shape of the  $S-N$  curve, the presentation of the fatigue lifetime inversion and the inversion number of cycles as well as the inversion range of stresses.

### CONCLUSIONS

Although characterization of the fatigue performance of materials is known to require a larger number of tests,

the limited data in this paper are mainly useful for a preliminary assessment of the fatigue characteristics of the material studied. More data are needed to clarify the fatigue behaviour of PEK-C. However, based on the present data and fracture surface observation, the following initial conclusions may be drawn.

In the tension-tension fatigue failure of injection moulded poly(phenylene ether ketone) (PEK-C), there are two different types of crack initiation and propagation: at higher cyclic stress levels the fatigue crack originates at one corner of the specimen and grows radially inward; at lower cyclic stress levels the fatigue crack nucleates at an internal defect of the specimen and grows radially outward. When the manner of crack initiation and propagation changes from one mode to the other, a lifetime inversion is observed from the  $S-N$  curve.

### ACKNOWLEDGEMENTS

The work reported in this paper was part of an exchange programme between the Chinese Academy of Sciences and the National Research Council of Italy. J. Zhou expresses his appreciation to the National Natural Science Foundation of China and Polymer Physics Laboratory, Chinese Academy of Sciences for the financial support. T. He is greatly indebted to the support of the National Outstanding Young Scientist Fund from



the Natural Science Foundation of China and the National Key Projects for Fundamental Research 'Macromolecular Condensed State', The State Science and Technology Commission of China.

## REFERENCES

- 1 Hertzberg, R. W. and Manson, J. A. 'Fatigue in Engineering Plastics', Academic Press, New York, 1980
- 2 Kenner, V. H. in 'Failure of Plastics' (Eds W. Brostow and R. D. Corneliussen), Hanser, New York, 1986, Chapter 3
- 3 Trotignon, J. P., Verdu, J., Martin, C. H. and Morel, E. *J. Mater. Sci.* 1993, **28**, 2207
- 4 Hwang, J.-F., Manson, J. A., Hertzberg, R. W., Miller, G. A. and Sperling, L. H. *Polym. Eng. Sci.* 1989, **29**, 1477
- 5 Wyzgoski, M. G., Novak, G. E. and Simon, D. L. *J. Mater. Sci.* 1990, **25**, 4501
- 6 Brillhart, M., Gregory, B. L. and Botsis, J. *Polymer* 1991, **32**, 1605
- 7 Takemori, M. T. *Polym. Eng. Sci.* 1988, **28**, 641
- 8 Brillhart, M. and Botsis, J. *J. Reinf. Plast. Compos.* 1993, **12**, 943
- 9 Zhang, H., Chen, T. and Yuan, Y. Chinese Patent 85108751.5, 1985
- 10 He, T. B., Li, B. Y., Zhang, Y. Z., Qu, G. J., Zhuang, Y. G., Chen, T. L., Yuan, Y. G., Qu, X. Z., Ding, M. X. and Lin, K. J. '7th ICCM Proceedings, Vol. 4' (Eds Wu Tunshu, Gu Zenlong and Wu Renjie), International Academic Publishers, Beijing, 1989, p. 40
- 11 Zhou, J., He, T. B., Li, B. Y., Liu, W. L. and Chen, T. L. *Compos. Sci. Technol.* 1992, **45**, 173
- 12 Han, Y. C., Yang, Y. M., Li, B. Y. and Feng, Z. L. *Makromol. Chem.* 1994, **219**, 125
- 13 Han, Y. C., Yang, Y. M., Li, B. Y. and Feng, Z. L. *J. Appl. Polym. Sci.* 1994, **54**, 375
- 14 Matsumoto, D. S. and Gifford, S. K. *J. Mater. Sci.* 1985, **20**, 4610
- 15 Takemori, M. T. *Polym. Eng. Sci.* 1987, **27**, 46
- 16 Hashemi, S. and Williams, J. G. *J. Mater. Sci.* 1985, **20**, 4202
- 17 Bandyopadhyay, S., Roseblade, T. R. and Muscat, R. *J. Mater. Sci.* 1993, **28**, 3777
- 18 Mandell, J. F., Smith, K. L. and Huang, D. D. *Polym. Eng. Sci.* 1981, **21**, 1173
- 19 Mandell, J. F. in 'Fatigue of Composite Materials' (Ed. K. L. Reifsnider), Elsevier, Amsterdam, 1990, Chapter 7